Atomic Glimpses on a Billion-Year-Old Molecular Machine

Eric Westhof* and Neocles Leontis

The ribosome is the universal molecular machine for the synthesis of proteins in biological cells. Each *Escherichia coli* cell contains about 30000 ribosomes. Eubacterial ribosomes are made up of two main components, each of which is composed of an intricate assembly of proteins and RNAs, totaling about 270000 atoms. In prokaryotes the small subunit (30S particle) comprises the 16S rRNA and 21 proteins, while the large subunit (50S particle) consists of two RNAs, the 5S rRNA, and the 23S rRNA, together with some 33 proteins.[1] Functionally, the small subunit is devoted to the recognition of messenger and transfer RNAs, while the large subunit is the center of protein synthesis. A prokaryotic ribosome measures about 200 Å along each direction, which corresponds to the close packing of approximately 16 nucleosomes, the fundamental constituent of chromatin. Recently, crystal structures of each prokaryotic subunit[2–4] and of the whole prokaryotic ribosome,[5] the 70S particle, have been published. The resolution of the structures is still rather low (4.5 – 7.8 Å; Table 1), but the prospects for a rapid increase in resolution are real.

Like all great endeavours in science, the quest for structural information on the ribosome has been eventful and ought to inspire ambitious young scientists, especially in days where science is shunned by students. The structures we can now admire were solved in the laboratories of scientists who have been involved in ribosome research for decades. Ada Yonath, from the Weizmann Institute in Rehovot, Israel, started first in the early 1980s, with the enthusiastic support of H. G. Wittmann at the Max-Planck-Institute für Molekulare Genetik in Berlin. Over the years, despite some open scepticism, Ada Yonath[6] persevered, incrementally improving the quality of the crystal structures by choosing to extract ribosomes from extreme halophilic and thermophilic bacteria and applying successive technical advances in X-ray crystallography (like cryocrystallography[7] to overcome radiation damage and synchroton radiation to surmount weak diffraction power). Her group has now published the structure of the 30S particle at 4.5 Å resolution.[2]

However, in the meantime, she had so successfully convinced fellow crystallographers of the feasibility of the project that other groups moved in, no longer content to study the structure of the ribosome piecemeal. Peter Moore, at Yale University, had deduced the relative positions of the proteins in the 30S subunit using neutron diffraction.[8, 9] This required over a decade of dedicated work since each single protein had to be isolated and purified in deuterated form before being reinserted singly or in pairwise combination with other proteins into reconstituted ribosomes. He teamed up with the well-known structural biologist Tom Steitz, also at Yale University, and their groups solved the structures of the 50S particle, first at 9 Å,[10] and then at 5 Å.[4] In parallel, Venki Ramakrishnan (first at the University of Utah in Salt Lake City and then at the Medical Research Council in Cambridge, UK), who had worked with Peter Moore on the relative positions of ribosomal proteins and, since then, solved the structure of several ribosomal proteins in isolated form,[11] has managed to produce a remarkable 5.5 Å resolution structure of the 30S particle with his group.[3] These two teams worked on crystals of isolated particles previously shown by Yonath's group to crystallize.[12, 13]

Since the mid 1980s, working in the group of the ribosome researcher A. Spirin (at the Protein Research Institute in Puschino, Russia), G. Yusupova and M. Yusopov worked to produce better and better crystals of a whole ribosome of a

Table 1. The different crystal structures which have been solved, together with their characteristics.

Particle	Size [MDa][a]	Contents[a]	Unit cell parameters [Å]	Space group	Resolution [Å] (no. of reflections)
30S *Thermus thermophilus*	0.9	16S rRNA (1542 nt), 21 proteins	$a=b=407$, $c=176$	$P4_12_12$	4.5 (85991),[2] 5.5[3]
50S *Haloarcula marismortui*[4]	1.6	23S rRNA (2900 nt), 5S rRNA (120 nt), 34 proteins	$a=212$, $b=301$, $c=576$	$C222_1$	5 (185190)
70S *Thermus thermophilus*[5]	ca. 2.5		$a=b=508$, $c=803$	$I422$	7.8 (121730)

[a] For *E. coli* ribosomes. nt = nucleotides.

[*] E. Westhof
Institut de Biologie Moléculaire et cellulaire du CNRS
UPR9002
15, rue René Descartes, 67084 Strasbourg-Cedex (France)
Fax: (+33) 3-88-417-066
E-mail: E.Westhof@ibmc.u-strasbg.fr
N. Leontis
Chemistry Department, Bowling Green State University
Bowling Green, OH 43403 (USA)

  0570-0833/00/3909-1587 $ 17.50+.50/0

thermophile.[14] They later brought their expertise in biochemistry and crystallogenesis to the laboratory of Harry Noller, a pioneer in the sequencing and characterization of ribosomal RNAs,[15–18] at the University of California in Santa Cruz. Noller's team, which had already been joined by Jamie Cate, who had previously participated in the ground-breaking structure of the P4-P6 domain of group I introns,[19] cracked the structure of the whole ribosome.[5]

Once the challenging difficulties of obtaining stable and well-diffracting crystals were overcome, crystallographers faced the tremendous problem of phasing the reflections diffracted by crystals containing such large asymmetric objects. The 30S particles were solved using the multiple isomorphous replacement method, with multimetal clusters[20] based on tantalum or tungsten, and anomalous scattering in one case[3] or oligomers modified by metal clusters and targeted to specific targets in the other.[2] For the 50S particle, the crystallographic problem was compounded by the fact that the crystals were twinned, but, again, multiple isomorphous replacement and multiwavelength anomalous scattering were used to phase at high resolution, once the phases at low resolution were obtained with the help of cryoelectron microscopy (cryo-EM).[10] The solution of the whole ribosome relied also on a battery of theoretical and experimental techniques: 1) several complexes of the 70S ribosome (with messenger RNA and transfer RNAs or analogues) were crystallized and measured in order to guarantee internal consistency; 2) low-resolution phases were determined using molecular envelopes derived from cryo-EM; and 3) extension of the phases to high resolution was achieved using multiwavelength anomalous dispersion experiments to locate heavy-atom clusters.[5]

The resolution, while not high enough to resolve and identify individual RNA bases or protein amino acids, is sufficient to distinguish protein α helices from RNA double helices, and thus the images reveal some of the overall arrangements of the proteins with respect to the RNAs. In the 1970s, to obtain the structures of tRNAs, crystallographers developed programs fitting the previously determined structures of RNA building blocks, phosphates, sugars, bases, and mononucleotides to the electron density of the tRNA polynucleotide.[21] To solve the present structures, whole domains—RNA helices, conserved hairpin stem-loops, recurrent RNA modules,[22, 23] and available complexes between RNA fragments and proteins[24, 25]—have to be recognized and fitted into the electron density. All seven 30S proteins that had been previously crystallized and solved to atomic resolution (S4, S5, S6, S7, S8, S15, and S17)[11] could be fitted in the electron density of the small subunit. Moreover, with the aid of data from the low-resolution neutron-scattering map[9] and biochemical experiments, the positions of some of the other 30S proteins could be identified (S2, S3, S11, S16, S18, and S20). In the large subunit, 12 proteins have been located. The atomic coordinates of five previously solved proteins (L1, L2, L6, L11, and L14) and two RNA fragments have been fitted to the electron density. Three of these proteins (L6, L11, and L14) and the two RNA fragments (the sarcin/ricin stem-loop and the L11-binding site of 23S RNA) comprise a major part of the binding site for G-protein factors.

Overall, the structures confirm clearly the beautiful reconstructions obtained by cryo-EM.[26–30] Thus, most of the features of the small subunit (head and neck connected to the platform and body; Figure 1) are discerned in the overall shapes with some modulations depending on the crystal and, importantly, the functional state of the particle. For the large subunit, some meaningful differences appear on the left- (L1) and right-hand (L7/L12) sides of the central protuberance (Figure 1) between the structures obtained by cryo-EM and crystallography. The cryo-EM images and biochemical data served also to dock the previously solved structures of the G-protein translation factors EF-G and EF-TU (complexed to aminoacyl-tRNA and GTP) to this site.[29, 30]

The synergism between these two experimental approaches has indeed great potential. This is illustrated by two recent developments.[31, 32] The insertion of a tRNA sequence within

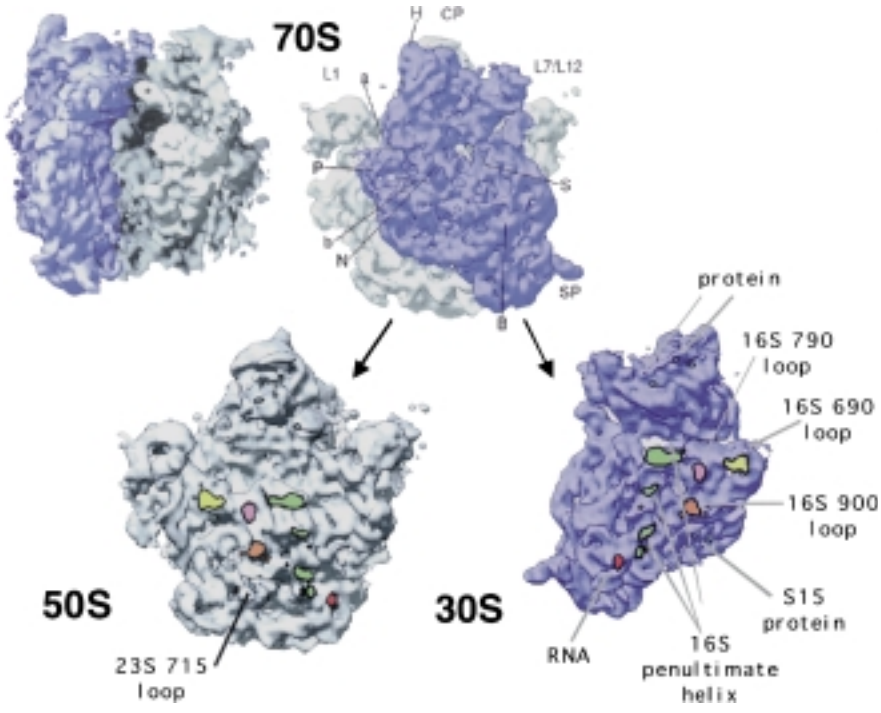

Figure 1. Interactions between the small (30S) and large (50S) ribosomal subunits participating in the formation of the functional 70S ribosome, as seen in the structure at 7.8 Å resolution. Top: Two views of the 70S particle, one edge-on and the other rotated by 90° to show the orientation of the 30S particle on the 50S particle. Bottom: The 70S particle is opened up to reveal the corresponding contact points on the two subunits. The contact points are color-coded and labeled to indicate the corresponding "bridges" first identified by cryoelectron microscopy, and the specific RNA hairpin loops or helices and ribosomal proteins now assignable at the higher resolution[41] (see also Table 2). The figure is adapted from Figures 2 and 3 of ref. [5] and used with permission from the American Association for the Advancement of Science (copyright (1999).

  0570-0833/00/3909-1588 $ 17.50+.50/0

the bacterial gene for the 23S rRNA allows the isolation of ribosomes with the L-shaped tRNA structure visible, thereby permitting the identification of specific regions within the whole particle.[31] The cryo-EM structure at 7.5 Å resolution of the *E. coli* 50S particle reveals new details concerning the L7/L12 region and the L8 complex as well as the extensive conformational changes occurring upon binding of the 30S particle.[32] The functional significance of the differences seen between X-ray and EM structures is now difficult to assess, but one expects large movements and rearrangements to occur within the ribosome during the cycles of protein synthesis (binding and release of tRNAs, progression along the messenger, extrusion of the synthesized peptide, etc.).[18]

Various examples of known RNA structural motifs are prominent in the areas of electron density (Figure 2). Firstly, most of the canonical double-helical elements can be identified as such, by following the regularly spaced "knobs" of electron density corresponding to phosphate groups. Secondly, hairpin loops capped by 5′-GNRA-3′ tetraloops can be identified, as these share a characteristic conformation, featuring continuous stacking of three bases (5′-NRA-3′).[33] Thirdly, several internal loops displaying characteristic S-motifs[34] have been identified, and two of these have been assigned to functionally significant regions in each subunit. One can be assigned to the 900 hairpin stem-loop in the small subunit (nucleotides 890–910 of 16S RNA, which includes the "switch-helix" at its base), and another to the sarcin/ricin hairpin stem-loop in the large subunit (nucleotides 2650–2670 of 23S RNA), which participates in translation-factor binding. Finally, multiple examples of RNA helices interacting side-by-side perhaps through "ribose zippers"[19] are observed. At the resolution of the present structures, however, single-stranded regions of RNA cannot be traced unambiguously over long distances. Nonetheless, the RNA backbone of 16S rRNA in the small subunit could be traced over most of the central core domain.[3] In addition, a conspicuous 100 Å long, slightly distorted RNA helix, seen in the 30S[2, 3] and 70S particles,[5] can be identified with the "penultimate" helix (residues 1400–1500) of 16S RNA. This functionally important domain includes the decoding site of 16S rRNA and forms a significant part of the interface to the 50S subunit, including bridges B2a, B3, and B5 (Table 2). Moreover it directly contacts the 900 hairpin stem-loop containing the S-motif and switch helix, which is implicated in modulating translation accuracy and which itself is seen to contact the 50S subunit at its hairpin loop (bridge B2c).

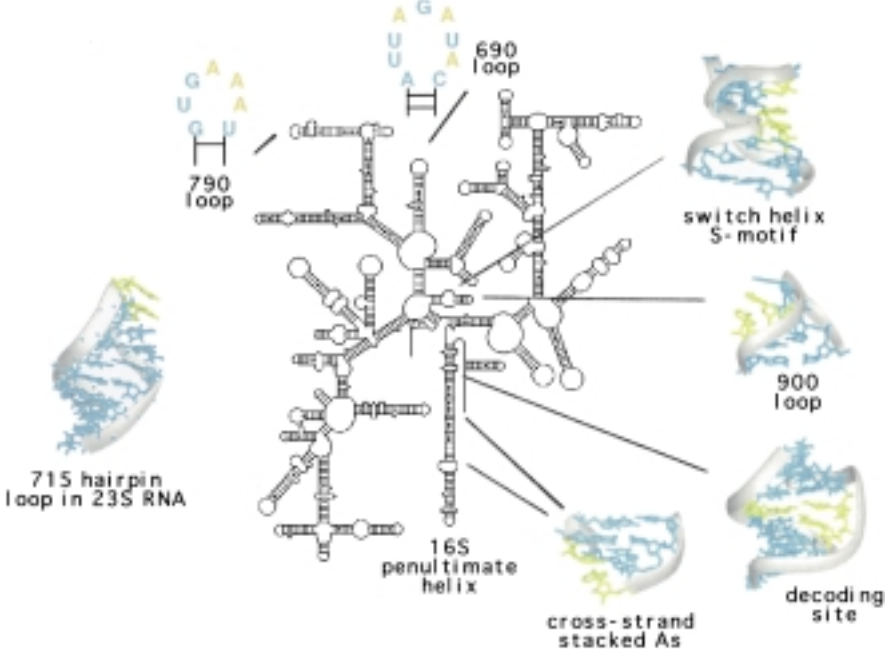

Figure 2. Some RNA elements participating in intersubunit interactions, mapped onto the secondary structure of the 16S ribosomal RNA. Conserved, exposed adenine residues, which are recurrently used in tertiary contacts,[46] are colored yellow.

What do the proteins do? An answer to this question is also emerging. The ribosomal proteins are dispersed throughout the structures of both subunits and most appear to cross-link noncovalently two or more RNA helices, a fact consistent with abundant data on chemical protection and cross-linking indicating that the same protein

Table 2. RNA–protein and RNA–RNA intersubunit contacts identified in the 70S eubacterial ribosome around the core region which bind mRNA and tRNAs.[5, 41] [a]

Contact	Type	Location	Small subunit	Large subunit
B1a	RNA–protein	peripheral	protein	RNA
B1b	RNA–protein	peripheral	protein	RNA
B4	RNA–protein	peripheral	S15 protein	715 RNA hairpin stem-loop
B6	RNA–protein	peripheral	RNA	protein
B2b	RNA–RNA	central core	790 hairpin stem-loop	RNA
B7	RNA–RNA	central core	690 hairpin stem-loop	RNA
B2c	RNA–RNA	central core	900 hairpin stem-loop	1700 hairpin stem-loop
B2a	RNA–RNA	central core	top PL-Sh.Gr.	1910 hairpin stem-loop
B3	RNA–RNA	central core	PL-Sh.Gr.	RNA
B5	RNA–RNA	central core	PL-D.Gr.	RNA

[a] The contact names were first established and named as "bridges" of electron density by cryoelectron microscopy.[41] PL corresponds to the penultimate helix in the 16S rRNA which carries the decoding site; the grooves of the RNA helix are denoted Sh.Gr. for the shallow, and broad, groove (corresponding to the minor groove in the B-DNA helix) and D.Gr. for the deep, and narrow, groove (corresponding to the major groove in B-DNA helix).

  0570-0833/00/3909-1589 $ 17.50+.50/0

contacts regions of the RNA distant in the primary or secondary structure. Thus, the general answer to the question is that the ribosomal proteins help to organize and stabilize the tertiary structural elements present in the RNAs. The organization of the RNA itself is built around a scaffold of RNA Watson–Crick helices connecting and positioning structural motifs, often recurrent and assembled from non-Watson–Crick base pairs,[35] with a diverse set of accessible binding sites. It is still much too early to discuss the relative contribution of RNA–protein and RNA–RNA contacts to the assembly of the subunits and the whole particle (see Table 2 for the present state of knowledge).

However, more direct functional roles for certain ribosomal proteins cannot be dismissed. In fact, the new structures reveal surprises, including the observation that proteins S5 and S4 in the small subunit interact directly, creating an interface that comprises the amino acids, which, when mutated, affect the ability of the ribosome to select the correctly aminoacylated tRNA (*ram* mutations). Furthermore, the structures are sufficiently detailed to reveal cavities and tunnels, some of which are used to bind and channel the substrates and products during the repetitive and highly processive cycle of protein synthesis. The presence of a channel leading from the active site of the peptidyl transferase straight through the body of the large subunit, and ascribed to the path of newly synthesized polypeptide, stands out in the structure of the 50S subunit. This tunnel, first suggested 30 years ago,[36] has been much discussed since it was seen in reconstruction models of the 50S and 70S particles.[37] Recently, cryo-EM provided evidence for its existence in yeast ribosomes.[38] It is 20 Å wide, 100 Å long, and filled by four W_{11} clusters in the 50S crystals.[4] Very striking is the almost complete absence of protein at the interface between the 30S and 50S subunits. It is at this interface that substrates are bound and peptide bond formation takes place. This pertains to the question: Is the ribosome a ribozyme or, in other words, is the RNA the chemically active component for catalysis of peptide bond formation? Although experimental evidence points to that possibility, definite proof is still missing.[39] Bridges representing points of contact between the subunits (Table 2) were first identified in lower resolution images obtained by cryo-EM.[40] On the basis of the present structure of the 70S subunit,[5] supplemented by additional biochemical work, an RNA–protein bridge spanning the subunit interface was identified as protein S15 of the 30S particle and the hairpin loop 715 in the 23S rRNA of the 50S particle.[41]

The new crystal structures crown decades of determined work and open up avenues for fundamental and applied scientific developments. The 16S ribosomal RNA has already played a central role in our classification of living forms. The subdivision of the tree of life into three main forms (archaea, eubacteria, and eukarya) was based on analysis of the sequences of 16S rRNAs.[42] Structurally, the ribosome is a gold mine of motifs and contacts. Extended comparisons between the three-dimensional structural motifs and the available sequences should yield the rules linking sequence and structure in RNA, as well as those responsible for RNA–protein recognition. The ribosome has been the subject of an intense modeling activity,[43] and thus the structures should help delineate the limits and future possibilities. Several antibiotics inhibit protein synthesis—either at the 50S level, like the macrolides, or at the 30S level, like the aminoglycosides—but organisms resistant to virtually any available antibiotic occur.[44] However, our knowledge at the atomic level of the antibiotic binding sites on the eubacterial ribosome is still scanty,[45] and we can now hope to see in the future complexes involving antibiotics. These will provide crucial new structural data to guide efforts in drug design necessary to overcome the imminent crisis in antibacterial therapy resulting from the spread of resistance.

[1] P. B. Moore, *Annu. Rev. Biophys. Biomol. Struct.* **1998**, *27*, 35–58.
[2] A. Tocilj, F. Schlünzen, D. Janell, M. Glühmann, H. A. Hansen, J. Harms, A. Bashan, H. Bartels, I. Agmon, F. Franceschi, A. Yonath, *Proc. Natl. Acad. Sci. USA* **1999**, *96*, 14252–14257.
[3] W. M. Clemons, Jr., J. L. May, B. T. Wimberly, J. P. McCutcheon, M. S. Capel, V. Ramakrishnan, *Nature* **1999**, *400*, 833–840.
[4] N. Ban, P. Nissen, J. Hansen, M. Capel, P. B. Moore, T. A. Steitz, *Nature* **1999**, *400*, 841–847.
[5] J. H. Cate, M. M. Yusupov, G. Z. Yusupova, T. N. Earnest, H. F. Noller, *Science* **1999**, *285*, 2095–2104.
[6] A. Yonath, *Annu. Rev. Biophys. Biomol. Struct.* **1992**, *21*, 77–93.
[7] H. Hope, F. Frolow, K. von Bohlen, I. Makowski, C. Kratky, Y. Halfon, H. Danz, P. Webster, K. S. Bartels, H. G. Wittmann, *Acta Crystallogr. Sect. B* **1989**, *45*, 190–199.
[8] M. S. Capel, D. M. Engelman, B. R. Freeborn, M. Kjeldgaard, J. A. Langer, V. Ramakrishnan, D. G. Schindler, D. K. Schneider, B. P. Schoenborn, I. Y. Sillers, *Science* **1987**, *238*, 1403–1406.
[9] M. S. Capel, M. Kjeldgaard, D. M. Engelman, P. B. Moore, *J. Mol. Biol.* **1988**, *200*, 65–87.
[10] N. Ban, B. Freeborn, P. Nissen, P. Penczek, R. A. Grassucci, R. Sweet, J. Frank, P. B. Moore, T. A. Steitz, *Cell* **1998**, *93*, 1105–1115.
[11] V. Ramakrishnan, S. W. White, *Trends Biochem. Sci.* **1998**, *23*, 208–212.
[12] A. Yonath, C. Glotz, H. S. Gewitz, K. S. Bartels, K. von Bohlen, I. Makowski, H. G. Wittmann, *J. Mol. Biol.* **1988**, *203*, 831–834.
[13] K. von Bohlen, I. Makowski, H. A. Hansen, H. Bartels, Z. Berkovitch-Yellin, A. Zaytzev-Bashan, S. Meyer, C. Paulke, F. Franceschi, A. Yonath, *J. Mol. Biol.* **1991**, *222*, 11–15.
[14] S. Trakhanov, M. Yusupov, V. Shirokov, M. Garber, A. Mitschler, M. Ruff, J. C. Thierry, D. Moras, *J. Mol. Biol.* **1989**, *209*, 327–328.
[15] H. F. Noller, C. R. Woese, *Science* **1981**, *212*, 403–411.
[16] H. F. Noller, J. Kop, V. Wheaton, J. Brosius, R. R. Gutell, A. M. Kopylov, F. Dohme, W. Herr, D. A. Stahl, R. Gupta, C. R. Woese, *Nucleic Acids Res.* **1981**, *9*, 6167–6189.
[17] H. F. Noller, *Annu. Rev. Biochem.* **1991**, *60*, 191–227.
[18] K. S. Wilson, H. F. Noller, *Cell* **1998**, *92*, 337–349.
[19] J. H. Cate, A. R. Gooding, E. Podell, K. Zhou, B. L. Golden, C. E. Kundrot, T. R. Cech, J. A. Doudna, *Science* **1996**, *273*, 1678–1685.
[20] J. Thygesen, S. Weinstein, F. Franceschi, A. Yonath, *Structure* **1996**, *4*, 513–518.
[21] J. L. Sussman, S. R. Holbrook, R. W. Warrant, G. M. Church, S. H. Kim, *J. Mol. Biol.* **1978**, *123*, 607–630.
[22] R. T. Batey, R. P. Rambo, J. A. Doudna, *Angew. Chem.* **1999**, *111*, 2472–2491; *Angew. Chem. Int. Ed.* **1999**, *38*, 2326–2343.
[23] P. B. Moore, *Annu. Rev. Biochem.* **1999**, *67*, 287–300.
[24] T. Hermann, E. Westhof, *Chem. Biol.* **1999**, *6*, R335-R343.
[25] D. E. Draper, *J. Mol. Biol.* **1999**, *293*, 255–270.
[26] A. Malhotra, P. Penczek, R. K. Agrawal, I. S. Gabashvili, R. A. Grassucci, R. Junemann, N. Burkhardt, K. H. Nierhaus, J. Frank, *J. Mol. Biol.* **1998**, *280*, 103–116.
[27] R. K. Agrawal, P. Penczek, R. A. Grassucci, J. Frank, *Proc. Natl. Acad. Sci. USA* **1998**, *95*, 6134–6138.
[28] R. K. Agrawal, P. Penczek, R. A. Grassucci, Y. Li, A. Leith, K. H. Nierhaus, J. Frank, *Science* **1996**, *271*, 1000–1002.

  0570-0833/00/3909-1590 $ 17.50+.50/0

[29] H. Stark, M. V. Rodnina, J. Rinke-Appel, R. Brimacombe, W. Wintermeyer, M. van Heel, *Nature* **1997**, *389*, 403 – 406.
[30] H. Stark, E. V. Orlova, J. Rinke-Appel, N. Junke, F. Mueller, M. Rodnina, W. Wintermeyer, R. Brimacombe, M. van Heel, *Cell* **1997**, *88*, 19 – 28.
[31] C. M. Spahn, R. Grassucci, P. Penczek, J. Frank, *Structure* **1999**, *7*, 1567 – 1573.
[32] R. Matadeen, A. Patwardhan, B. Gowen, E. V. Orlova, T. Pape, M. Cuff, F. Mueller, R. Brimacombe, M. van Heel, *Structure* **1999**, *7*, 1575 – 1583.
[33] C. C. Correll, A. Munishkin, Y. L. Chan, Z. Ren, I. G. Wool, T. A. Steitz, *Proc. Natl. Acad. Sci. USA* **1998**, *95*, 13436 – 13441.
[34] C. C. Correll, I. G. Wool, A. Munishkin, *J. Mol. Biol.* **1999**, *292*, 275 – 287.
[35] Review: N. B. Leontis, E. Westhof, *Q. Rev. Biophys.* **1998**, *31*, 399 – 455.
[36] L. I. Malkin, A. Rich, *J. Mol. Biol.* **1967**, *26*, 329 – 346.
[37] A. Yonath, K. R. Leonard, H. G. Wittmann, *Science* **1987**, *236*, 813 – 816.
[38] R. Beckmann, D. Bubeck, R. Grassucci, P. Penczek, A. Verschoor, G. Blobel, J. Frank, *Science* **1997**, *278*, 2123 – 2126.
[39] R. Green, C. Switzer, H. F. Noller, *Science* **1998**, *280*, 286 – 289.
[40] J. Frank, A. Verschoor, Y. Li, J. Zhu, R. K. Lata, M. Radermacher, P. Penczek, R. Grassucci, R. K. Agrawal, S. Srivastava, *Biochem. Cell Biol.* **1995**, *73*, 757 – 765.
[41] G. M. Culver, J. H. Cate, G. Z. Yusupova, M. M. Yusupov, H. F. Noller, *Science* **1999**, *285*, 2133 – 2136.
[42] W. E. Balch, L. J. Magrum, G. E. Fox, R. S. Wolfe, C. R. Woese, *J. Mol. Evol.* **1977**, *9*, 305 – 311.
[43] R. Brimacombe, *Eur. J. Biochem.* **1995**, *230*, 365 – 383.
[44] R. M. Anderson, *Nat. Med.* **1999**, *5*, 147 – 149.
[45] D. Fourmy, M. I. Recht, J. D. Puglisi, *J. Mol. Biol.* **1998**, *277*, 347 – 362.
[46] L. Ortoleva-Donnelly, A. A. Szewczak, R. R. Gutell, S. A. Strobel, *RNA* **1998**, *4*, 498 – 519.

How Does Tyrosinase Work? Recent Insights from Model Chemistry and Structural Biology**

Heinz Decker,* Renée Dillinger, and Felix Tuczek*

Introduction

The catalysis of oxygenation and oxidation reactions by tyrosinase and catecholoxidase is currently one of the most exciting topics of bioinorganic chemistry. These enzymes belong to the family of type 3 copper proteins which is involved in a variety of biological functions. Hemocyanins (Hcs) serve as O_2 carriers in the hemolymph of arthropods and molluscs,[1] catecholoxidases (COases) oxidize *ortho*-diphenols to *ortho*-quinones (diphenolase activity),[2] and tyrosinases mediate the hydroxylation of monophenols to *ortho*-diphenols as well as the subsequent oxidation to *ortho*-quinones (monophenolase activity).[3] Although they have been studied for over 100 years, these reactions and the observed functional differences are far from being understood on a molecular level.

[*] Prof. Dr. H. Decker
Institut für Molekulare Biophysik
Johannes Gutenberg Universität Mainz
Jakob Welder Weg 26, 55128 Mainz (Germany)
Fax: (+49) 6131-3923557
E-mail: decker@biophysik.biologie.uni-mainz.de
Prof. Dr. F. Tuczek, Dipl.-Chem. R. Dillinger
Institut für Anorganische Chemie
Christian Albrechts Universität Kiel
Olshausenstrasse 40, 24098 Kiel (Germany)
Fax: (+49) 431-8801520
E-mail: ftuczek@ac.uni-kiel.de

[**] This work was supported by the Medicine and Science Center of the University of Mainz (H.D.) and the Deutsche Forschungsgemeinschaft (F.T., R.D.). The authors thank M.Möller for help with the graphical artwork.

With the notable exception of tyrosinase, X-ray structures are available for all classes of type 3 copper proteins: the deoxy form of the Hc from spiny lobster (*Panulirus interruptus*),[4] the deoxy and oxy forms of the Hc from horseshoe crab (*Limulus polyphemus*),[5] the oxy form of the Hc from *Octopus dofleini*,[6] and the deoxy, met, and inhibitor-bound forms of the COase from sweet potato (*Ipomoea batatas*).[7] As expected, all of these proteins contain virtually the same binuclear copper active site which in its $Cu^I - Cu^I$ deoxy form reversibly binds O_2, leading to a binuclear Cu^{II} unit with O_2 as a side-on bridging (μ-η^2:η^2) peroxide group. Based on these structural data, a mechanistic understanding of the corresponding biochemical reactions now appears within reach. In this respect, the recent finding of mono- and diphenolase activity in activated Hcs[8] is of great interest, as it provides information regarding the orientation of monophenolic substrates within the protein pocket containing the binuclear copper active site.

Importantly, the growing structural insight into COase and tyrosinase activity is complemented by a significant amount of chemical and mechanistic information obtained from the study of synthetic low molecular weight analogues.[9] The current electronic-structural, spectroscopic, and chemical characterisation of the Cu_2O_2 cores present in these inorganic model systems constitutes a fascinating area of bioinorganic research in itself and will most probably be crucial for a further understanding of the oxygenation reactions mediated by tyrosinase. The present highlight first describes key results of these model studies and these are then contrasted with mechanistic proposals derived from structurally characterized proteins.

  0570-0833/00/3909-1591 $ 17.50+.50/0